Slope Stability Evaluation for the New Railway Embankment using Stochastic Finite Element and Finite Difference Methods

Eleyas Assefa*

Doctoral Candidate
China Three Gorges University, Yichang, Hubei 443002, China.
** Corresponding author e-mail:eleyas@ctgu.edu.cn*

Dr. Li Jian Lin

Professor
China Three Gorges University, Yichang, Hubei 443002, China.

Dr. Costas I. Sachpazis

Associate Professor, Civil & Geotechnical Engineer, BEng(Hons) Civil Eng. UK, Dipl Geol, M.Sc. Eng. UK, Ph.D. NTUA, Post-Doc. UK, Gr.m.ICE, Greece.

Dr. Deng Hua Feng

Professor
China Three Gorges University, Yichang, Hubei 443002, China.

Dr. Sun Xu Shu

Associate Professor
China Three Gorges University, Yichang, Hubei 443002, China.

Xiaoliang Xu

China Three Gorges University, Yichang, Hubei 443002, China

ABSTRACT

Evaluation of Slope stability is one of the day-to-day practices of geotechnical engineers. Nowadays, different methods are available to evaluate the stability of a particular slope. Despite the advances that have been made in site exploration, evaluating the stability of slopes remains a challenge. Recently, Ethiopia has been trying to construct a newly planned railway routes to connect the country's development centers and link with ports of neighboring countries. However, this newly planned railway routes will pass in the heart of highly fragile mountainous terrains and earthquake prone regions. Therefore, the prime objective of this paper is to investigate the stability of the railway embankment by using three different stochastic approaches (First Order Reliability Method, Point Estimate Method and Monte Carlo Simulation) with commercially available finite element and finite difference programs. Moreover, the seismic response of the railway

embankment was studied by using a nonlinear analysis (FLAC2D v 7.0) program. The first order reliability method (FORM), Monte Carlo Simulation (MCS) and Point-estimate method (PEM) gave 3.2%, 4.14% and 1.5% of probability of failure respectively. In the mean time, there was no any indication of liquefaction observed due to stiff foundation clay soils and deep groundwater table.

KEYWORDS: Slope Stability Analysis; Slope Failure; Soil Properties; Uncertainty; Embankment Loading Conditions; Finite Element Method; Finite Difference Method

INTRODUCTION

Evaluation of Slope stability is one of the day-to-day practices of geotechnical engineers. Nowadays, different approaches are available to evaluate the stability of a particular slope [1], [2], and [3]. Despite the advances that have been made, evaluating the stability of slopes remains a challenge [4], [5], [6], and [7]. The fundamental requirement for stability of slopes is that the shear strength of the soil must be greater than the shear stress required for equilibrium [1] and [2]. If the shear stress exceeds the shear strength of the soil, different forms of slope failure will occur [8], [9], [10], and [11].

Recently, Ethiopia has been trying to construct a newly planned railway routes to connect the country's development centers and link with ports of neighboring countries. However, this newly planned railway routes will pass in the heart of highly fragile mountainous terrains and earthquake prone regions. Previously, the authors of this paper [12] did a probabilistic slope stability evaluation for the new railway embankment found in Ethiopia, using Quake/w and Slope/w programs. In their study, several different conditions, reflecting different stages in the life of the new railway embankment were simulated. The long term and short term stability of the railway embankment were investigated. The corresponding factors of safety were 2.585 and 2.199 respectively. Moreover, three different approaches were applied to scrutinize the effect of earthquake on the stability of the railway embankment. The pseudo-static analyses were done by using the conventional approach (the corresponding factor of safety was 1.221) and the effective stress approach (the corresponding factor of safety was 1.656). Then Newmark's deformation analysis was carried out [12]. The factor of safety (1.695) was obtained by using the results of Quake/w analysis into slope/w program. Finally, the sensitivity study on the railway embankment revealed that the shear strength parameters of the silty-clay foundation soil (layer-II) will govern the stability of the railway embankment. The previous study was based on the limit equilibrium (LE) slope stability analysis. However, it is important to point out that, limit equilibrium methods cannot provide the lower bound. But, sometimes it will furnish lower factor of safety than the one computed by using the finite element (FE) methods [13]. In this case one should not rely up on the LE solution.

Therefore, the prime objective of this paper is to investigate the stability of the previously studied railway embankment [12] by implementing three different stochastic approaches (First Order Reliability Method, Point Estimate Method and Monte Carlo Simulation) into commercially available finite element and finite difference programs. To meet this objective, only pseudo-static analysis was chosen to perform the stochastic analysis, in view of the fact that pseudo-static analysis gave the minimum factor of safety for this particular railway embankment [12]. If the strength of the soil is reduced less than 15 percent by cyclic loading, pseudo-static analyses of the earthquake loading can be used [1]. However, some engineers perform dynamic analysis for all slopes, even if the strength reduction due to earthquake loading is less than 15 percent [1]. Knowing that, dynamic analyses are very complex, involve considerable uncertainties, and are if the strength of the soil is reduced more than 15 percent as a result of cyclic loading, dynamic analyses are needed to estimate the deformations that would result from earthquakes [1]. Despite its simplicity, pseudo-static analyses produced factor of safety above 1 would fail during earthquakes [1], [14], and [15]. This shows the

inability of pseudo-static method to reliably evaluate the stability of slopes susceptible to weakening instability (Liquefaction). Regarding to this, there have been tremendous works to evaluate the liquefaction susceptibility of fine grained soils [16], [17], [18], [19], [20], [21], [22], [23], [24], and [25]. Nonetheless, there is no universally acceptable guideline to evaluate the liquefaction potential of fine grained soils. As it was discussed by Prakash [26], "It is obvious that it is still not possible to evaluate the likelihood of liquefaction of silts or silty clays with the same confidence as for clean sands without additional investigations". For this reason, the seismic response of the railway embankment was studied by using a nonlinear analysis (FLAC2D v 7.0). The standard practice for dynamic analysis of earth structures, and especially analyses dealing with liquefaction, is based primarily upon the equivalent-linear method. The nonlinear numerical method has not been applied as often in practical design [13]. However, the equivalent-linear method takes drastic liberties with physics, but is user-friendly and accepts laboratory results from cyclic tests directly [13]. The fully nonlinear method correctly represents the physics, but demands more user involvement and needs a comprehensive stress-strain model in order to reproduce some of the more subtle dynamic phenomena.

METHODS AND MATERIALS

Project Location

Awash – Kombolcha – Hara Gebaya Railway Project is a 390 km long railway (Figure 1a) between cities of Awash (km 0), Kombolcha (~km 270) and Hara Gebaya (~km 390). Currently, this railway project is under ongoing construction. Previously, the authors of this paper [3] suggested the method of analyses to be adopted for the newly planned railway routes in Ethiopia. In this paper, a particular critical high fill railway embankment at Km 261+140 was chosen for the stability analyses. This railway embankment is located in close proximity to Kombolcha city (Ethiopia). Figure 1b shows typical railway embankment fill on the specified site.

Figure 1a: Newly planned railway routes **Figure 1b:** Typical railway embankment

Soil Properties

The soil strata at km 261+140 are mainly composed of over-consolidated cohesive soils ranging from stiff to very stiff clay soils. Important geotechnical properties of the railway embankment and the foundation materials are shown in Table 1. After careful extrapolation of the ground water table from the nearby boreholes, the groundwater table was estimated (11m from the ground surface), and the expected surcharge load on the embankment was 15kPa [12].

When the cohesion of embankment soil specified as zero, the minimum factor of safety will always tend towards the infinite slope case. Moreover, the critical slip surface will be parallel and immediately next to the slope face [27]. To overcome such situation and to get a more realistic slip surface, soil suction was considered. For many years the significance of suction has never been quantified [28]. According to Fredulund [28], the suction in an unsaturated soil increases the cohesion of the soil. Accordingly, the shear strength parameters used in a slope stability analysis should be modified to reflect the in-situ soil suction condition. Fredulund [28] suggested that the suction of a soil could be considered as an increase in cohesion. Considering the relationship among pore radius, matric suction, and capillary height, the cohesion of the embankment material was defined to as 5kPa.

Table 1: Geotechnical properties of the railway embankment

Parameters	Fill	Silty clay (layer I)	Silty clay (layer II)	Silty clay (layer III)	Rock
Thickness (m)	14	2	11.5	8.1	8.4
γ uns (kN/m3)	20	18	18	18	20
γ sat (kN/m3)	20	18	18	18	20
E(kPa)	50,000	15,000	17,000	25,000	300,000
υ	0.25	0.35	0.35	0.35	0.25
Cu (kPa)	-	100	100	100	-
C (kPa)	0	20	20	20	20
ϕ	40	26	26	26	42
Vs (m/s)	-	177	303	389	811
G(kPa)	20,000	5,555.6	6,296.3	9,259.3	120,000
K(kPa)	33,333.3	16,666.7	18,888.9	27,777.8	200,000
porosity	0.3	0.3	0.3	0.3	0.3

Shear Strength Reduction Approach

Finite element and finite difference methods have wide application in geotechnical engineering. Specially, with the development of computers these method have been increasingly used and they have been a popular tool to evaluate the stability of slopes [1], [29], and [30]. Some of the advantages of finite element approach over the limit equilibrium methods in the analysis of slope stability problems were given by Griffiths and Lane, 1999 [30]. Unlike limit equilibrium approach, finite element method doesn't require any Prior assumptions about the location, direction and shape of the failure surface [1] and [2]. In the mean time, FEM can accurately determine stress, strains and the corresponding shear strengths. It is a powerful tool to monitor the progressive failure [1]. However, it has also drawbacks relative to the limit equilibrium methods. For instance, lack of complex models and the difficulty of incorporating some features like tension cracks and reinforcement in the stability model [1]. Slope stability evaluation using finite element and finite difference methods can be done by using the strength reduction approach [29], [30], [31], [32], [33], [34], and [35]. In this technique, the shear strength of the material will be artificially reduced till a state of limiting equilibrium

achieved. The method is commonly used with Mohr-Coulomb failure criterion. The safety factor F is defined according to the following equations.

$$C^{trial}=\frac{1}{F^{trial}}C \quad (1)$$

$$\phi^{trial}=\tan^{-1}\left(\frac{1}{F^{trial}}\tan\phi\right) \quad (2)$$

Pseudo-static Analysis

As it was mentioned previously, if the strength of the soil is reduced less than 15 percent by cyclic loading, *pseudo-static* analyses of the earthquake loading can be used [1]. In this analysis a unidirectional pseudo-static acceleration was applied through the sliding mass. Considering the previous study [12], a peak ground acceleration of 0.3g for 10% probability of occurrence in 50 years was opted for the analysis. Although engineering judgment is required for all cases, the criteria of Hynes-Griffin and Franklin (1984) should be appropriate for most slopes [1]. Therefore, using the criteria provided by Hynes-Griffin and Franklin (1984) [36]; an acceleration multiplier factor of 0.5 and 80% of the static shear strength were used for the pseudo-static analysis. Moreover, the pseudo-static analysis was done by using effective stress approach (the one suggested by Marcuson (1990)) [37], where excess pore water pressures are used to represent the post-earthquake strengths, effective stress shear strength parameters and excess pore water pressures are used in lieu of undrained shear strengths for the first-stage analysis.

Slope Stability Evaluation using stochastic approach

Uncertainty and risk are central features of geotechnical and geological engineering. Engineers can deal with uncertainty by ignoring it, by being conservative, by using the observational method, or by quantifying it [6]. In recent years, the uses of reliability analysis and probabilistic methods have been increasing in geotechnical engineering and related fields [1] and [6]. In the past, several researchers conducted slope stability analysis by using probabilistic approach [30], [38], [39], [40], [41], [42], [43], and [44].

Central problem facing the geotechnical engineer is to establish the properties of soils and rocks that will be used in the analysis, whether that analysis is probabilistic or deterministic [45]. However, to develop a reliable design approach, one must use statistical methods to deal with the variability of input parameters.

In this study, among the most commonly used methods; First Order Reliability Method (FORM), Monte-Carlo Simulation (MCS) and Point–Estimate Methods (PEMS) were used together with commercially available finite element and finite difference programs, to study the stability of the rail way embankment under pseudo-static analysis. Some of the advantages and disadvantages of these methods have been discussed in detail by Christian and Baecher (2003) [6].

The N-Sigma Rule

In this particular site, fissures or cracks were observed in the clay deposits. Some of the fissures were several meters in length and depth, especially in areas with deep groundwater table. Therefore, both sample recovery and strength testing were very difficult on these fissured clays. In this situation, testing of an intact sample may give an unrealistically high strength, and fissured sample unrealistically low strength. Therefore, considerable engineering judgment was required to derive the design parameters. Similarly, in geotechnical engineering the values of soil properties are frequently estimated based on correlations or on meager data plus judgment [1], [46], and [47], and it is not possible to use the standard deviation equation to determine the standard deviation. However, the N-

Sigma rule (Foye 2006) [48] provides a means of taking into account the fact that an engineer's experience and available information. N-Sigma rule is expressed as follows:

$$N_\sigma = \frac{H_{cv} - L_{cv}}{N_\sigma} \quad (3)$$

where: H_{cv} and L_{cv} are the highest and lowest conceivable values of the parameter respectively. According to [1] a better estimate of standard deviation would be made by dividing the range by 4. This conclusion (i.e., N_σ=4) was made based on the works of Christian and Baecher (2001) [49].

As it was mentioned in the introduction part, the sensitivity study [12] on the railway embankment revealed that the shear strength parameters of the silty-clay foundation soil (layer-II) will govern the stability of the railway embankment. Therefore, the shear strength parameters of the foundation soil (layer II) were considered as random variables. Based on Hynes-Griffin and Franklin (1984) criteria, 80% of the static shear strength parameters were determined, and these values were defined as the most likely values for the pseudo-static analysis. Then N-sigma rule was used to compute the standard deviations of the random variables (4kPa for the cohesion and 4.26 degree for the internal angle of friction) as shown in Table 2.

Table 2: Determination of standard deviation for foundation soil (layer II) based on the Nσ rule

Silty-clay foundation soil (layer II)	LCV	HCV	MLV*	σ	COV
Cohesion (kPa)	8	24	20*0.8=16	4	0.25
Angle of friction (degree)	12.8	29.85	tan-1(0.8*tan 26)=21.31	4.26	0.2

*most likely value (M_{LV})

Furthermore, the computed coefficients of variations (COV) in Table 2 have been compared with the existing literatures [6] and [50], and they were found in a good agreement with the published data. Both cohesion and internal angle of friction were assumed as statistically independent parameters. As it is well known, many natural data sets follow a bell-shaped distribution and measurements of many random variables appear to come from population frequency distributions that are closely approximated by a normal probability density function. This is also true for many geotechnical engineering material properties. Figure 2a and 2b represented the assumed probability density function for the random variables.

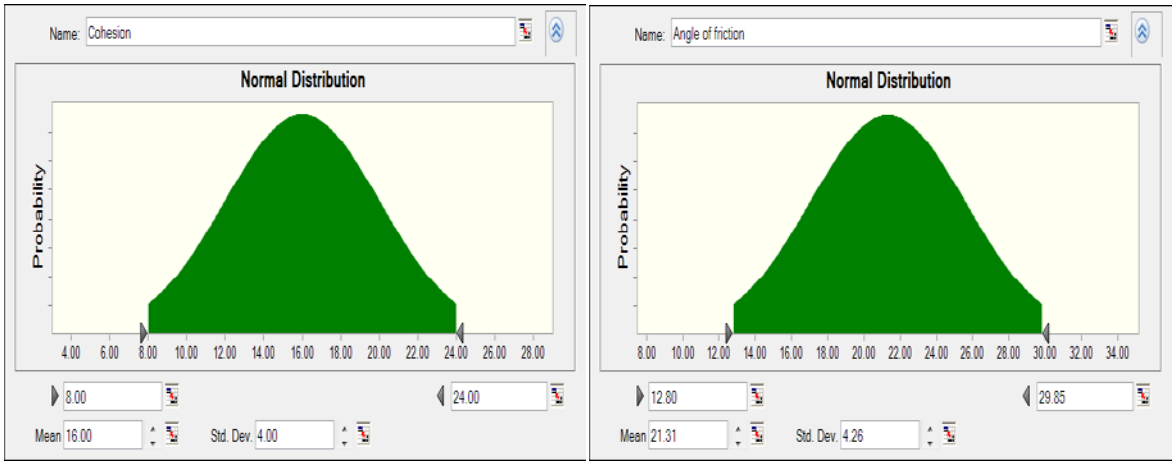

Figure 2a: PDF for cohesion **Figure2b:** PDF for internal angle of friction

First Order reliability Method

First Order Reliability Method (FORM) is the simplest and the most widely used method, started by assuming that all the $(x_i - \mu_{xi})$ terms are small, so their squares, cubes, and higher powers will be even smaller, and can be ignored [51]. Since only the first order terms are included, methods based on this assumption are called First Order Reliability Method (FORM).

In this paper, the algorithm, suggested by Rackwitz and Fiessler (1978) [51] was adopted to conduct the pseudo-static slope stability analysis for the railway embankment. This method linearizes the performance function at each iteration point; and uses the derivatives to find the next iteration point. Compared to other nonlinear optimization algorithms available in the literature, the algorithm just described requires the least computation at each step. The next iteration point is computed using a single recursive formula that requires information only about the value and the gradient of the performance function. The storage requirement is therefore minimal. The algorithm is also found to converge fast in many cases [51]. The procedures used in this method are described herein under.

Step 1: Define the appropriate performance function.

Step 2: Assume initial values of the design point:x_i^*, i=1, 2,…, n, and compute the corresponding value of the performance function *g( )*. In the absence of any other information, the initial design point can be the mean values of the random variables.

Step 3: Compute the mean and standard deviation at the design point of the equivalent normal distribution for those variables that are not normal.

$$x_i'^{*} = \frac{x'_{i-\mu_{X_i}^N}}{\sigma_{X_i}^N} \tag{4}$$

Step 4: Compute the partial derivatives $\frac{\partial g}{\partial x_i}$ evaluated at the design point x_i^*.

Step 5: Compute the partial derivatives $\frac{\partial g}{\partial x_i'}$ in the equivalent standard normal space.

Step 5: Compute the partial derivatives $\frac{\partial g}{\partial x_i'}$ in the equivalent standard normal space.

$$\frac{\partial g}{\partial x_i'} = \frac{\partial g}{\partial x_i}\sigma_{X_i}^N \tag{5}$$

The components of the corresponding unit vector are the direction cosines of the performance function, computed as

$$\alpha_i = \frac{\left(\frac{\partial g}{\partial X_i}\right)^* \sigma_{X_i}^N}{\sqrt{\sum_{i=1}^n \left(\frac{\partial g}{\partial X_i}\sigma_{X_i}^N\right)^{2*}}} \quad (6)$$

Step 6: Compute the new values for the design point in the equivalent standard normal space ($x_i'^*$) using the following recursive formula:

$$x_{k+1}'^* = \frac{1}{|\nabla g(x_k'^*)|^2}[\nabla g(x_k'^*)^t - g(x_k'^*)]\nabla(x_k'^*) \quad (7)$$

Where: $\nabla g(x_k'^*)$ is the gradient vector of the performance function, at $x_k'^*$, iteration point. Note that k refers to the iteration number. Therefore $x_k'^*$ is a vector with components$[x_{1k}'^*, x_{2k}'^*, \dots, x_{nk}'^*]^t$, where n is the number of random variables.

Step 7: Compute the distance (β) to this new design point from the origin.

$$\beta = \sqrt{\sum_{i=1}^n (x_i'^*)^2} \quad (8)$$

Check the convergence criterion for β(Δβ ≤0.005).

Step 8: Compute the new values for the design point in the original space (x_i^*) as

$$x_i^* = \mu_{X_i}^N + \sigma_{X_i}^N x_i'^* \quad (9)$$

And compute the value of the performance function g () for the new design point, check g () is very close to zero within 0.005. If both convergence criterions satisfied stop the computation, otherwise, repeat Steps 3 through 8 until convergence. To evaluate the partial derivatives of the performance function, central finite difference method was used as:

$$\left(\frac{\partial g}{\partial c}\right)^* = \frac{f(c^*+\Delta c,\emptyset^*)-f(c^*-\Delta c,\emptyset^*)}{2\Delta c} \quad (10$$

Where: c^* and $\emptyset^*$ are values of shear strength parameters at the design point. Here, Δc was defined as 10percent of the standard deviation of cohesion (i.e., Δc=0.1*4=0.4). The factor of safety of the railway embankment was evaluated at $(c^* + \Delta c, \emptyset^*)$ and $(c^* - \Delta c, \emptyset^*)$. Then the partial derivatives of the performance function were easily determined.

$$\left(\frac{\partial g}{\partial \emptyset}\right)^* = \frac{f(c^*,\emptyset^*+\Delta\emptyset)-f(c,\emptyset^*-\Delta\emptyset)}{2\Delta\emptyset} \quad (11)$$

Where: Δ∅ was defined as 10percent of the standard deviation of internal angle of friction (i.e., Δ∅ =0.1*4.26=0.426)

Monte Carlo simulation Using FLAC 2D v7.0

In contrast to the traditional limit equilibrium codes, FLAC provides a full solution of the coupled stress/ displacement, equilibrium and constitutive equations. In FLAC the failure surface is delineated by the concentration of shear strain contours. In this study, a fine-grid model was used, since it can clearly define the shear strain contours. Then, the pseudo-static slope stability analysis was done by implementing a Monte Carlo simulation into FLAC.

The Monte Carlo Simulation (MCS) is a powerful and popular tool for the evaluation of uncertainties in engineering practices [52] and [53]. It can be applied for both correlated and un-correlated random variables [54]. However, the number of simulations can affect the accuracy of the technique. In this paper, Box and Muller [55] algorithm was used to generate a pair of random deviates from the same normal distribution starting from a pair of random numbers.

Let U_1, U_2 be independent random variables from the same rectangular density function on the interval (0, 1). Consider the random variables:

$$x_1=(-2\log_e U_1)^{1/2} \cos(2\pi U_2) \quad (12)$$

$$x_2=(-2\log_e U_1)^{1/2} \sin(2\pi U_2) \quad (13)$$

$$x_i = \mu_x + N_i\sigma_x \quad (14)$$

Then (x_1, x_2) will be a pair of independent random variables from the same normal distribution with mean zero, and unit variance. The normal variables were determined by using the mean and standard deviation.

A FISH program was written to generate probabilistic input variables and their random combinations were used to perform a number of deterministic computations. Outliers of shear strength parameters have been excluded during the analysis. Beside, a mean factor of safety for the railway embankment was determined by using the mean shear strength parameters. The failure criterion was defined in terms of nodal unbalanced force ratio. If the unbalanced force ratio is less than 10^{-3} after N steps, then the system is in equilibrium [13]. However, if the unbalanced force is greater than 10^{-3}, then it will be considered as a failure. The following flowchart (Figure 3) clearly demonstrates the procedures used in the analysis.

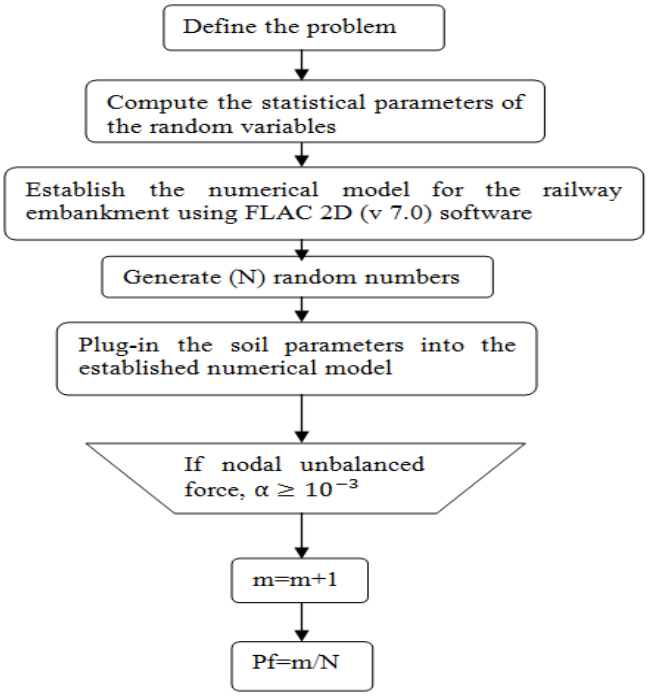

Figure 3: Flow chart for Monte Carlo Simulation used in FLAC2D program

The probability of failure for the railway embankment was computed by using the ratio of the total number of failures to the total number of Monte Carlo simulations. Finally, the standard deviation of safety factors was determined by using the Z-table together with Equation (15).

$$Z = \frac{x-\mu}{\sigma} \quad (15)$$

Where x is the variable of interest μ is the mean, and σ is the standard deviation.

Reliability index (β) was determined by using the following equation.

$$\beta=\frac{\mu-1}{\sigma} \quad (16)$$

Point Estimate Method using Phase^2 v8.0

The point estimate method was performed, by using the commercially available finite element program (Phase^2 v8.0). This program has been used in the design and analysis of mining, tunneling and surface excavations. However, few applications have been reported in the area of slope stability analysis [56]. The slope stability analysis for the railway embankment was done by using the strength reduction factor (SRF) approach. Phase^2 v8.0 enables the user to carry out a probabilistic slope stability analysis based on the Rosenblueth two-point-estimate method, for the first and the second moment of uncorrelated variables. Though the two-point-estimate method is easy to use and satisfactorily accurate for a range of practical problems, it has also some detriments [6]. The main limitation of this method is that, it deals with normal distribution only. The other constraint is, even if all the inputs follow normal distributions the outputs may not be normally distributed and the point estimate method approximation can be inaccurate. Figure 4 shows the stepwise procedures used during the analysis. The factors of safety were evaluated by using four different combinations (Figure 4).

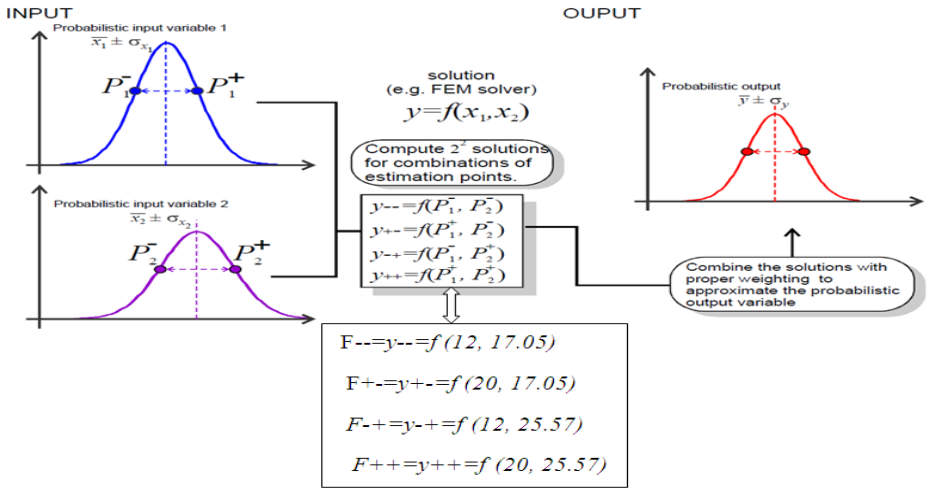

Figure 4: Computation principle of two point estimate method used in phase^2 v 8.0

Dynamic Analysis of the railway embankment

Estimation of Representative Material Properties

In this analysis, the foundation and embankment soils were modeled as elastic-perfectly plastic Mohr-Coulomb materials. The geotechnical properties of the railway embankment are listed in Table 1. Average relationships between the dynamic shear moduli and damping ratios of soils, as functions of shear strain and static properties, have been published for various soil types [57]. Therfore, the dynamic characteristics of all of the soils in this model were assumed to be governed by the modulus reduction factor (G/Gmax) and damping ratio (λ) curves, as shown in Figure 5.

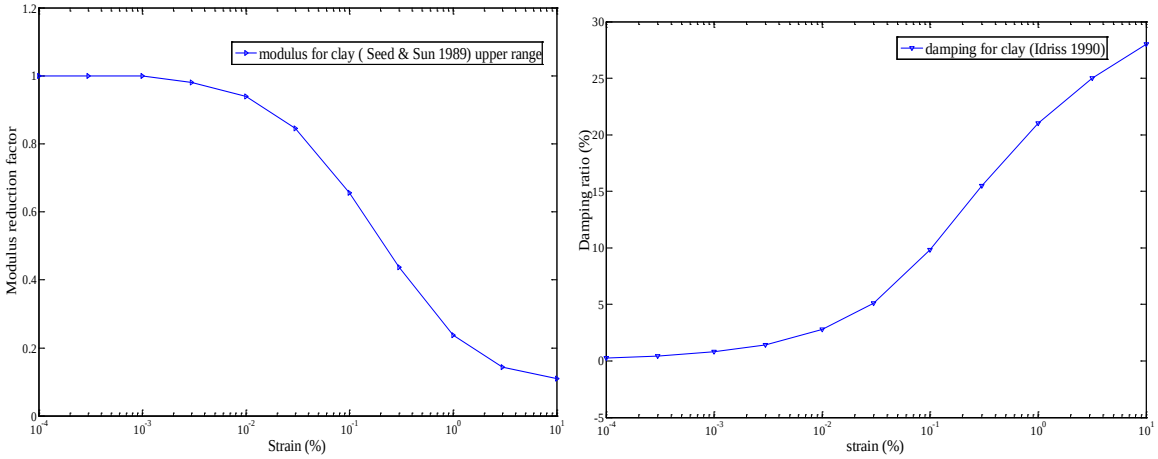

(a) Modulus reduction curve for Clay (b) Damping ratio curve for Clay

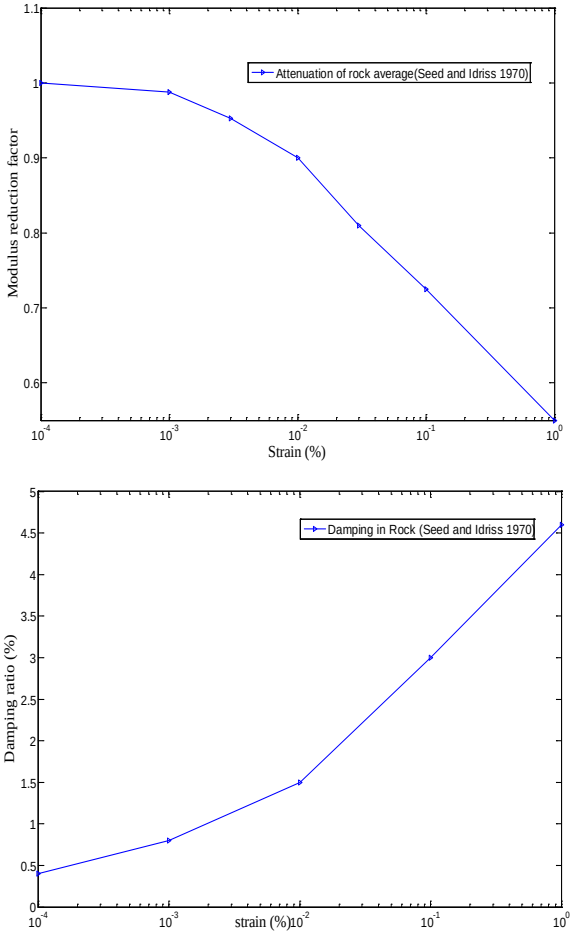

(c) Modulus reduction curve for Rock (d) Damping ratio curve for Rock

Figure 5: Dynamic characteristics of the soil/ Rock used in Shake2000 model Rayleigh Damping Parameters

The equivalent linear program SHAKE2000 was run to estimate the Rayleigh damping parameters to represent the inelastic cyclic behavior of the soils in the FLAC model, based upon the curves in Figure 5. A SHAKE2000 free-field column model was created for the foundation soils as shown in Figure 6. The second and the third layers in the free-field column were subdivided into 5 and 3 equal sub layers (Table 3). Similarly, the rock layer was subdivided into two sub layers.

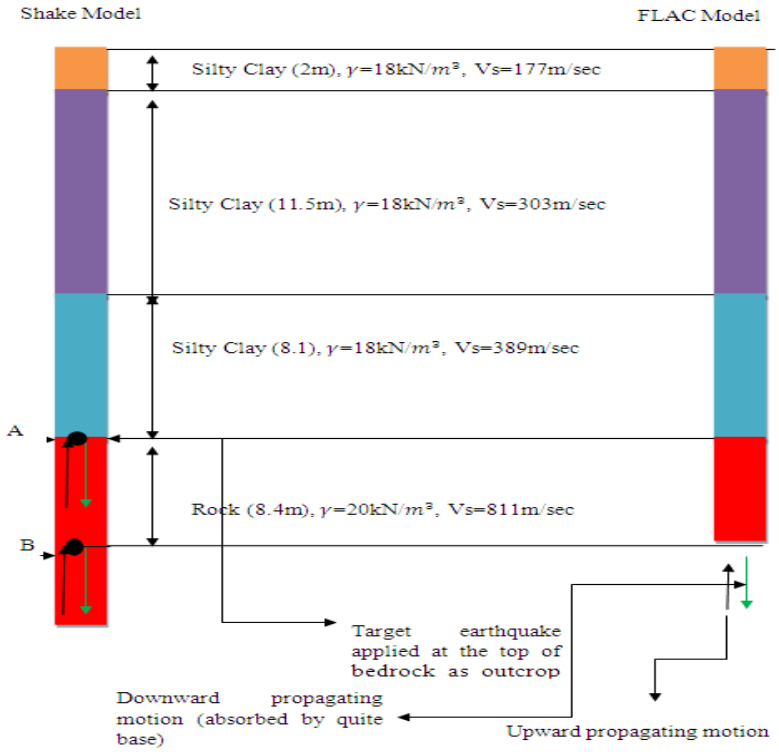

Figure 6: Compliant base deconvolution procedure

The SHAKE2000 analysis was performed using the shear wave speeds, densities, and modulus-reduction and damping-ratio curves for the foundation soils, and the target earthquake motion (The 1940 El Centro (California) earthquake acceleration time history was scaled to the peak ground acceleration of 0.3g to represent the study area) specified for the site. A nominal material damping of 0.1% was used for all layers in order to minimize approximations introduced by the Rayleigh damping model employed in the FLAC analysis (Rayleigh damping is frequency dependent).

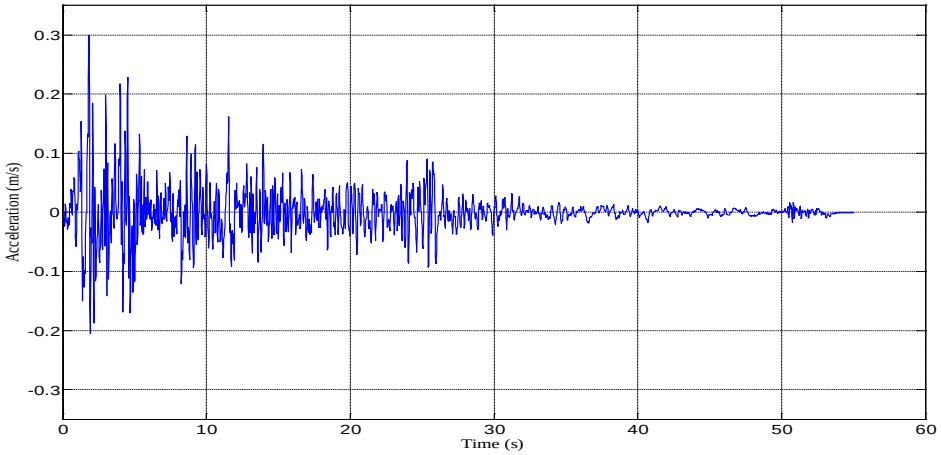

Figure 7: Target earthquake motion applied at the top of bedrock (M=6.7)

Strain-compatible values for the shear-modulus reduction factors and damping ratios throughout the soil column were determined from the analysis. Average modulus-reduction factors and damping ratios were then estimated for the foundations soils based upon the values calculated by SHAKE-2000 and the results are listed in Table 3.

Table 3: Strain compatible damping and modulus reduction for the foundation soil (Shake2000 results)

Thickness (m)	Uniform strain (%)	New Damping	G/Gmax
2.0	0.01918	0.042	0.885
2.3	0.01997	0.042	0.882
2.3	0.03578	0.058	0.819
2.3	0.05183	0.072	0.760
2.3	0.06531	0.081	0.724
2.3	0.07460	0.087	0.703
2.7	0.04140	0.064	0.796
2.7	0.04208	0.064	0.793
2.7	0.04482	0.067	0.783
4.2	0.00854	0.015	0.907
4.2	0.00878	0.015	0.906

Damping ratio and modulus-reduction parameters were selected corresponding to the equivalent uniform strain (which is taken as 50% of the maximum strain) for each layer [13]. The maximum equivalent uniform strain for the foundation soils was defined as 0.075%, the weighted damping ratio and weighted modulus reduction factor were determined as follows:

Weighted damping ratio:

$$= \frac{(2*.042+2.3*.042+2.3*.058+2.3*.072+2.3*.081+2.3*.087+2.7*.064+2.7*.064+2.7*.067+4.2*.015+4.2*.015)}{30}$$

= 0.051

Weighted G/Gmax:

$$= \frac{(2*.885+2.3*.882+2.3*.819+2.3*.760+2.3*.724+2.3*.703+2.7*.796+2.7*.793+2.7*.783+4.2*.907+4.2*.906)}{30}$$

= 0.82

The above computed values (damping ratio and modulus-reduction factor) were used as an input for the Rayleigh damping runs in the established FLAC model.

Water Bulk Modulus

In a coupled flow problem, the true diffusivity is controlled by the stiffness ratio R_k (i.e., the stiffness of the fluid versus the stiffness of the matrix):

$$R_k = \frac{k_{w/n}}{k+4G/3} \tag{17}$$

Where: K_w is the water bulk modulus, n is the porosity, and k and G are the bulk and shear moduli of soil.

The water bulk modulus can be reduced such that R_k = 20 without affecting the results significantly (and reducing the simulation time). Considering the minimum value of shear moduli for layer I, the value of K_w has been adjusted as shown below.

$$R_k = \frac{k_{w/0.3}}{16666.7+4*5555.6/3} = 20 \xrightarrow{yields} k_w = 144444.8\text{kPa}$$

Liquefaction Properties

The liquefaction condition was estimated for the foundation soil (layer II) in terms of standard penetration test results. Average standard penetration number (12.5) for layer II was taken as a normalized standard penetration test value, $(N_1)60$. For a normalized SPT blow count of 12.5, the Finn-Byrne model parameters were C_1 = 0.371 and C_2 = 1.078. Figure 8 shows the borehole log at chainage 261+130.

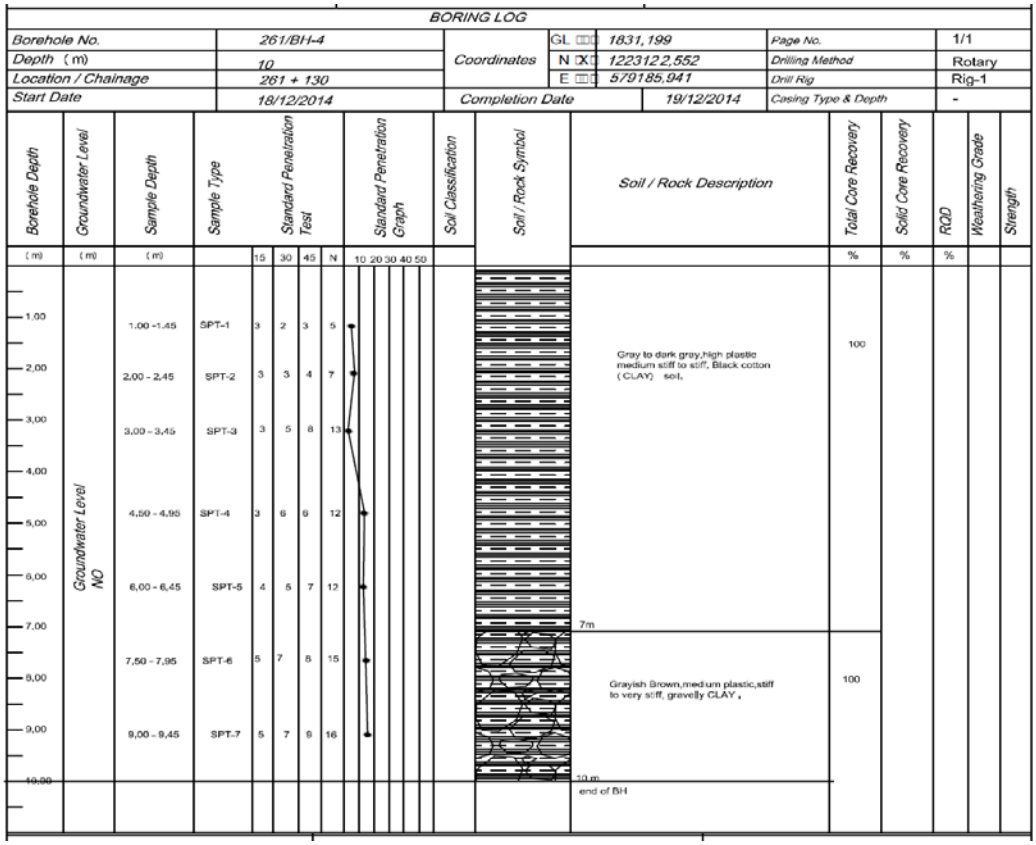

Figure 8: Borehole log at chainage 261+130

Deconvolution Analysis and Estimation of Seismic Motion Characteristics

The deconvolution procedure used in this paper is presented in Figure 6. For the compliant base case there is actually no need to include the soil layers in the SHAKE model as these will have no effect on the upward propagating wave train between points A and B [58]. In this particular case, it is not really necessary to perform a formal deconvolution analysis. This is because the upward propagating motion at point B will be almost identical to that at point A. Apart from an offset in time; the only differences will be due to material damping between the two points, which will generally be small for bedrock [58]. Thus, for this very common situation, the correct input motion for FLAC is simply ½ of the target motion (Figure 9).

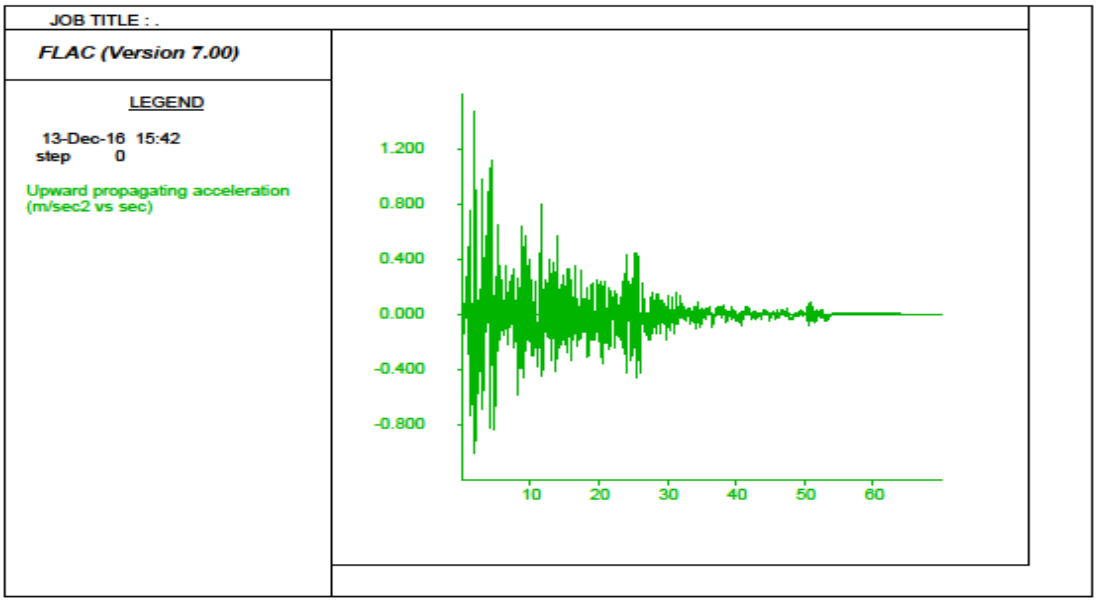

Figure 9: Upward propagating motion (1/2 of the target motion)

A fast Fourier transform (FFT) analysis of the input acceleration record results in a power spectrum as shown in Figure 10. As it can be seen (Figure 10) ,the dominant frequency was approximately 1Hz, the highest frequency component was less than 10 Hz, and the majority of the frequencies are roughly less than 5 Hz. Then the input acceleration was filtered to remove frequencies above 5 Hz (by using the FISH function "FILTER.FIS"). In the mean time, the input record was also checked for baseline drift. The FISH function "INT.FIS" was used to integrate the velocity record again to produce the displacement waveform related to the input acceleration. Then, a baseline correction was performed by adding a low frequency sine wave to the velocity record. And noisy data from the input acceleration were trimmed off at 50 second.

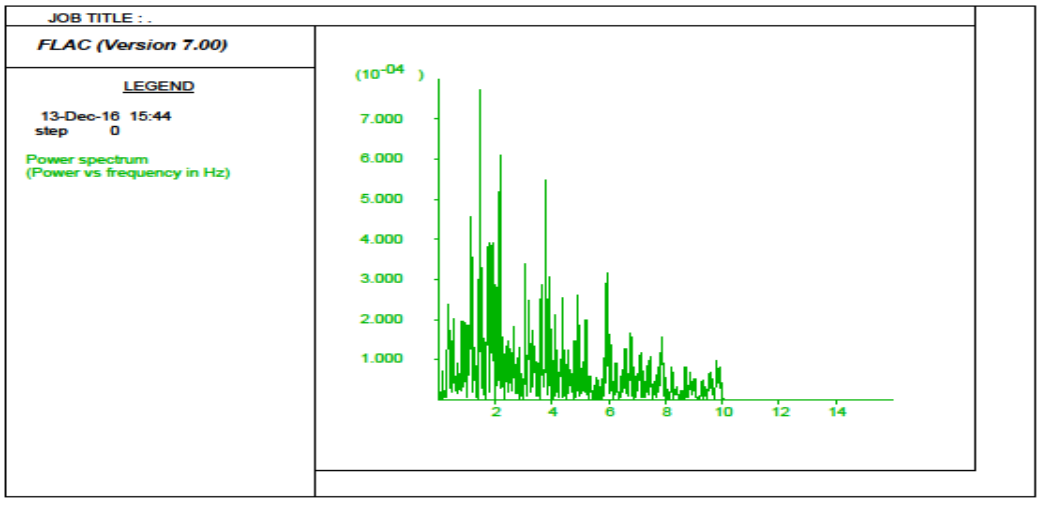

Figure 10: Power spectrum of upward propagating motion (acceleration time history)

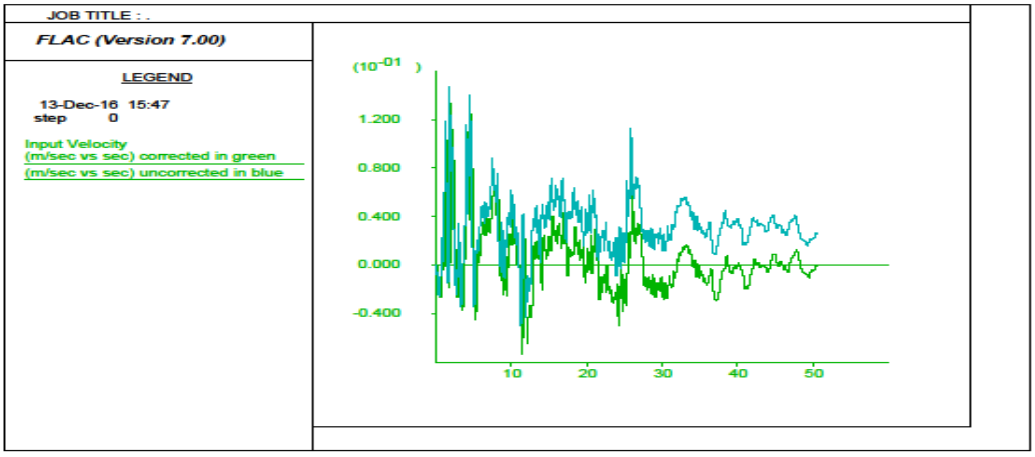

Figure 11: Input velocity used in FLAC with 5Hz filter and baseline correction

Adjust Input Motion and Mesh Size for Accurate Wave Propagation

The mesh size for the FLAC model was selected to ensure accurate wave transmission. Based upon the elastic properties listed in Table 1, embankment soil layer I has the lowest shear wave speed (177 m/sec). The model used in the analysis has 60 by 19 quadrilateral-zone meshes as shown in Figure 12. The largest zone size in the FLAC model was found to be 2.4m. Then the maximum frequency that can be modeled accurately was:

$$f=\frac{Cs}{10\Delta L}\approx 7.4\text{Hz} \tag{18}$$

As it was previously mentioned, before applying the acceleration input record, it was filtered to remove frequencies above 5 Hz.

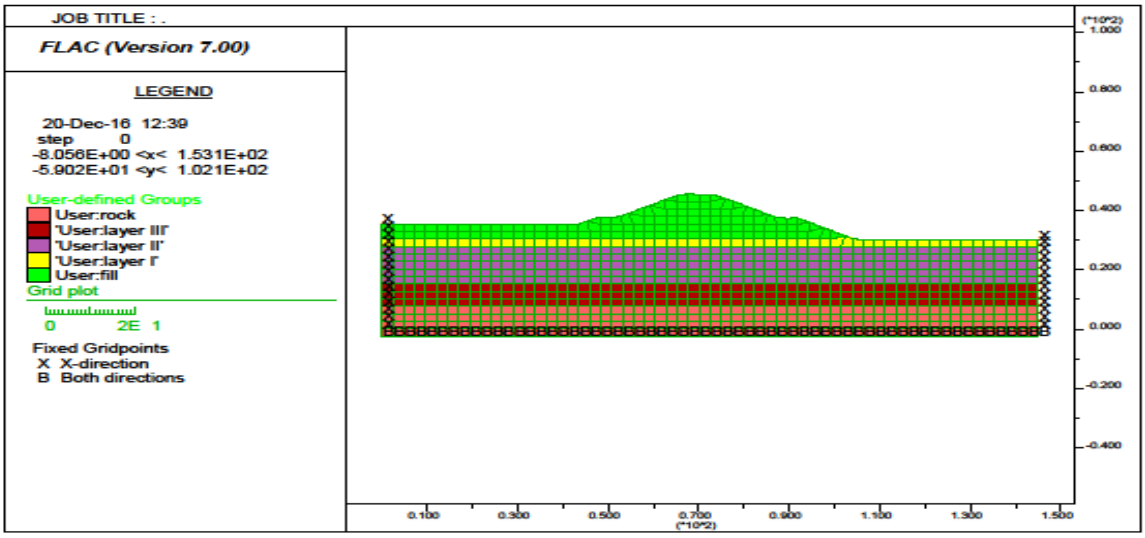

Figure 12: Railway embankment model with foundation and embankment soils assigned

Initial state of stress

The analysis was started from the state before the embankment is constructed. Roller boundaries are assigned along the sides of the model, and a fixed boundary along the base was assigned. A fish function ininv was employed to compute the pore pressures and stresses automatically for a model containing a phreatic surface. The function requires the phreatic surface height (wth = 19 for this railway embankment) and the ratios of horizontal to vertical effective stresses (assumed to be k0x = k0z = 0.5). The pore pressure, total stress and effective stress distributions were then calculated automatically. The equilibrium state was checked (using the SOLVE elastic option in the Run/Solve tool).

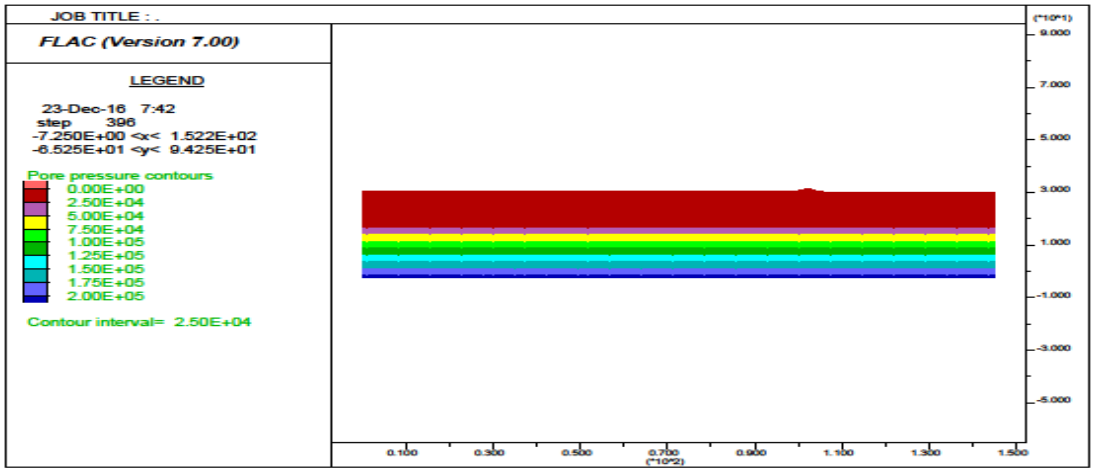

Figure 13: Pore pressure distribution in foundation soils

In this particular railway embankment, the generation of excess pore-pressures and the associated possible liquefaction were not a critical issue at this site, due to the clay foundation and deep groundwater table. Therefore, the embankment was placed in one stage. In addition to the embankment, a surcharge load of 15kPa was introduced into the FLAC model, and the model was run in small-strain mode. This state was considered to be state of the embankment dam at the time of the earthquake event. Then the factor of safety of the railway embankment at this stage was computed.

Dynamic Loading Conditions

For the dynamic loading stage, pore pressures can change in the materials due to dynamic volume changes induced by the seismic excitation. The filtered and baseline-corrected input velocity was called into the established FLAC model. The free-field boundary was set for the side boundaries and a compliant boundary condition was assumed for the base. The dynamic wave was applied as a shear-stress boundary condition along the base after specifying the density, shear wave velocity of the base material and multiplying it by the provided input velocity.

Simulation with Rayleigh Damping

The parameters for the Rayleigh damping model were chosen based on the SHAKE2000 analysis, as it was previously discussed. The initial shear modulus was reduced by a factor of 0.82, and the damping ratio of 0.051was used. The center frequency for Rayleigh damping was 1.0 Hz, as determined from the input wave. The FISH function “GREDUCE.FIS” was executed to reduce the elastic moduli by 0.82 factor.

Seismic Calculation Assuming Liquefaction

Liquefaction is one of important, interesting, complex, and controversial topics in geotechnical earthquake engineering [14]. Fine grained soils (silts and clays) are vulnerable to liquefaction under certain circumstances [26]. There have been a significant controversy and confusion regarding to the liquefaction potential of fine grained soils, as it was pointed out by Seed [20]. Similarly, Prakash [26] signified the deficiency of universally acceptable guidelines to evaluate the liquefaction susceptibility of fine grained soils.

In this analysis, the foundation soil (layer II) was changed to liquefiable material. The Finn-Byrne liquefaction model was prescribed for the foundation soil (layer II), the parameters used for this model was described previously. Cyclic pore-pressure ratio (u_e /σ'_c), was used to identify the likelihood of liquefaction on the foundation soil. Where u_e is the excess pore-pressure and σ'_c is the initial effective confining stress. Note that a liquefaction state is reached when $u_e / \sigma'_c = 1$.

RESULTS AND DISCUSSIONS

Figure 14 clearly shows the maximum shear strain contours for the railway embankment, using the mean shear strength parameters and pseudo-static analysis. At this stage the mean factor of safety was determined as 1.24. According to Hynes-Griffin and Franklin (1984) [1] criteria the minimum factor of safety for ~1m tolerable displacement is 1.0. Therefore, the mean factor of safety of the railway embankment complied with the specified criteria.

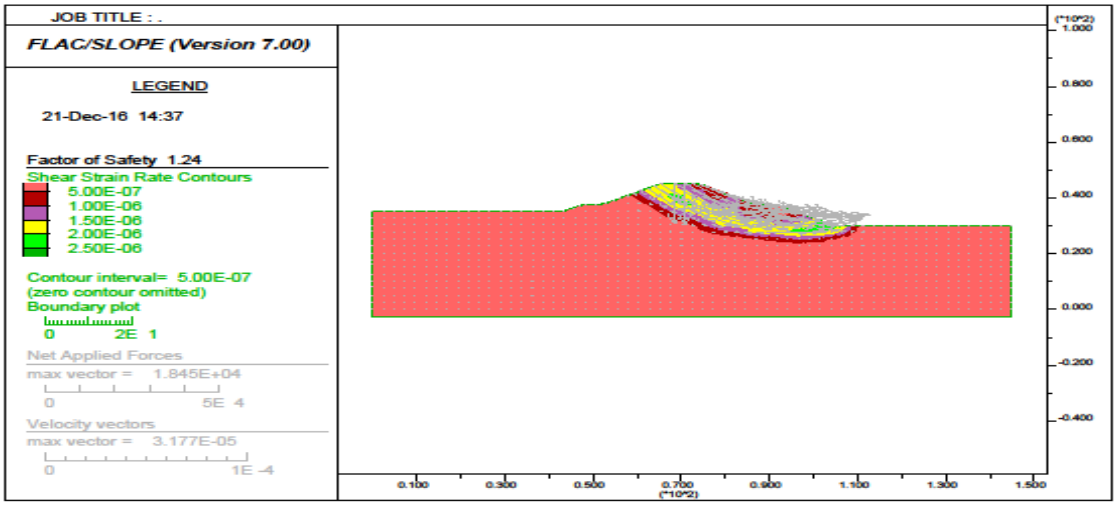

Figure 14: Maximum shear strain contours (Pseudo-static mean factor of safety)

Moreover, similarities in the failure surfaces between FLAC (Figure 14) and slope/w (Figure 15) programs have been observed.

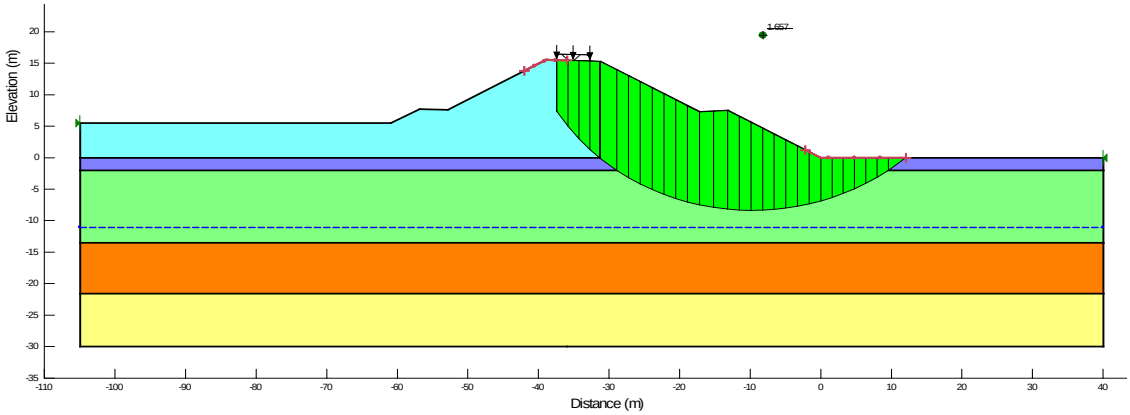

Figure 15: Pseudo-static analysis using effective stress approach and Slope/w [12]

In concept, any slope with a factor of safety above 1.0 should be stable. However, in practice the level of stability is seldom considered acceptable unless the factor of safety is significantly greater than 1.0. This is just to compensate the combined effects of uncertainties in the parameters involved in the slope stability analysis. The reliability of a slope is an alternative measure of stability that considers explicitly the uncertainties involved in the stability analysis. Reliability analysis is an important tool for quantifying uncertainties in geotechnical engineering. Factor of safety and reliability are complement to each other. In this paper, the reliability or probability of failure of a railway embankment was evaluated by using three different stochastic approaches. The results of each method are discussed and presented separately.

Probability of failure using FORM

In this pseudo-static analysis, the random variables (shear strength parameters) were considered as normally distributed and statistically independent parameters. The performance function was defined as *g()=F-1=0*. Where: F is a factor of safety. The stability analysis was done by using FLAC2D program. Each run was done by increasing and reducing the variables by 10 percent of the standard deviation of the corresponding variables. Then central finite difference method was used to evaluate the partial derivatives of the performance function at the design point. The results of this method are tabulated in Table 4. The reliability index (β) for the railway embankment was found to be 1.85 (Table 4). The mean factor of safety (1.24) was determined deterministically by using the mean shear strength parameters of the railway embankment. Then the respective standard deviation was determined after employing Equation 16 as follows:

1.85=$\frac{1.24-1}{\sigma}$, solving for the unknown parameter yielded, σ =0.1297.

Then Equation 15 was used to get the z value as shown below,

$z = \frac{(1-1.24)}{0.1297}$=-1.85

Hence, the probability of failure (3.2%) was determined by using the above result (z=-1.85) together with the Z-Table.

Table 4: Steps used in FORM

Step 1	Defined performance function g()=F-1=0, where F is factor of safety.				
Step 2	Initial values : c^*=16, $\emptyset^*$=21.3, and g()=0.24				
Step 3	$\mu^N c$	16	16	16	16
	$\sigma^N c$	4	4	4	4
	$\mu^N \emptyset$	21.3	21.3	21.3	21.3
	$\sigma^N \emptyset$	4.26	4.26	4.26	4.26
	c'^*	0	-0.706	-0.5216	-0.5838
	$\emptyset'^*$	0	-2.824	-1.9210	-1.7560
Step 4	$\left(\frac{\partial g}{\partial c}\right)^*$	0.005	0.0146	0.01463	0.015
	$\left(\frac{\partial g}{\partial \emptyset}\right)^*$	0.0188	0.0505	0.04132	0.03
Step 5	$\left(\frac{\partial g}{\partial c'}\right)^*$	0.02	0.0584	0.05852	0.06
	$\left(\frac{\partial g}{\partial \emptyset'}\right)^*$	0.080	0.2151	0.17602	0.1278
Step 6	New C'^*	-0.706	-0.5216	-0.5838	-0.7868
	New $\emptyset'^*$	-2.824	-1.9210	-1.7560	-1.6759
Step 7	New β	2.910	1.99	1.851	1.851
	Δβ		0.92	0.139	0.000
Step 8	New c^*	13.176	13.914	13.665	12.853
	New $\emptyset^*$	9.269	13.117	13.819	14.161
	New g()	-0.205	-0.0254	0.00195	0.00195

Probability of failure using Monte Carlo simulation

The Monte Carlo simulation (MCS) is considered as a very powerful tool for the design and analysis of engineering schemes. In this method, samples of probabilistic input variables were generated and their random combinations were used to perform a number of deterministic computations. However, the accuracy of MCS depends on the number of simulations used in the analysis. To capture this phenomenon, a numerical experiment was conducted. The result showed that, the probability of failure was almost steady while the number of simulations exceeded 1000 (Figure 16a). Therefore in this study, the probability of failure was determined by using 5000 MCS, and it was found to be 4.14%. Then the standard deviation (0.1384) was computed by using Equation 15 and Z-table together. Moreover, the reliability index (β) was evaluated by using Equation 16 as shown below.

$$\beta = \frac{\mu - 1}{\sigma}$$

$$= \frac{1.24-1}{0.1384} = 1.73$$

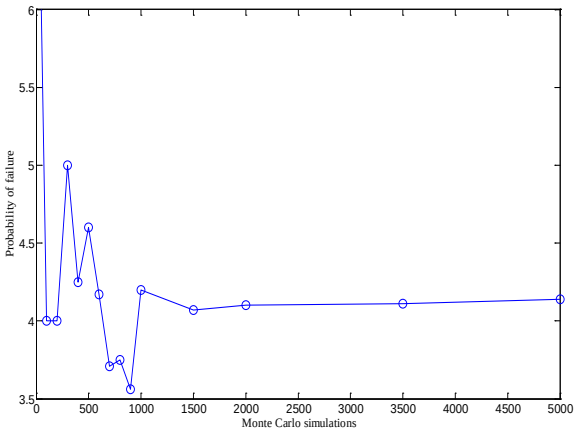

Figure 16a: MCS vs. Probability of failure

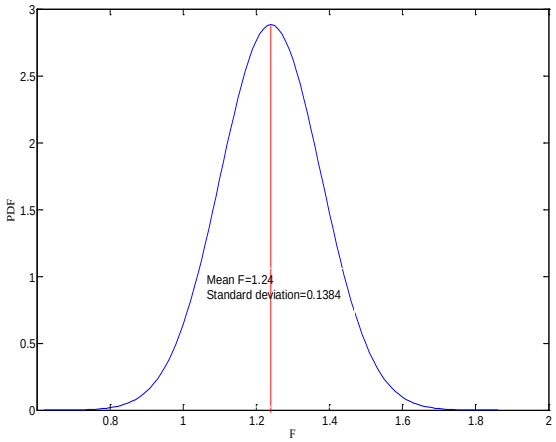

Figure 16b: Normal distribution of F.

Since the variability of the soil properties is normally distributed, the probability density function of the factor of safety is also expected to be normally distributed. Therefore, the probability distribution was plotted with MATLAB as shown in Figure 16b.

MCS doesn't require the knowledge of optimization skills, as required by the first-order reliability methods (FORM); and it is mostly general and robust to the dimension of random variables and problem complexity. Nowadays, with the development of powerful personal computers its problem related to time can be minimized.

Probability of failure using Point Estimate Method

Finite element analysis are often computing time intensive and are not well-suited for the multiple runs needed for systematic sensitivity analyses or statistical simulations (eg. Monte Carlo). However, Point estimate method (PEM) is straightforward, easy to use, and requires little knowledge of probability theory. Therefore, the pseudo-static analysis for the railway embankment was carried out by using a built-in simple computing efficient probabilistic method in phase^2 finite element program. Based on the results of the analysis (Figure 17), the probability of failure was found to be 1.5%. Similarly, the mean factor of safety and the standard deviation were 1.16 and 0.0714 respectively.

While the point-estimate method is popular in practice, it has many detractors. A great limitation of the point-estimate method for multiple variables is that it requires calculations at 2^n points. When n is greater than 5 or 6, the number of evaluations becomes too large for practical applications, even in the day of cheap computer time. The other limitation is, even if all the inputs follow normal distributions the outputs may not be normally distributed and the PEM can be inaccurate [6]. This occurs especially when different behaviors are occurring (e.g. elasticity and plasticity). Besides, the very simplicity of the method suggests to some that the answer is overly approximate. It is worth noting that, two points may not be adequate to obtain accurate estimates of the moments for the function Y in a particular case [6]. Despite these limitations, the method remains a simple, direct, and effective method of computing the low-order moments of functions of random variables.

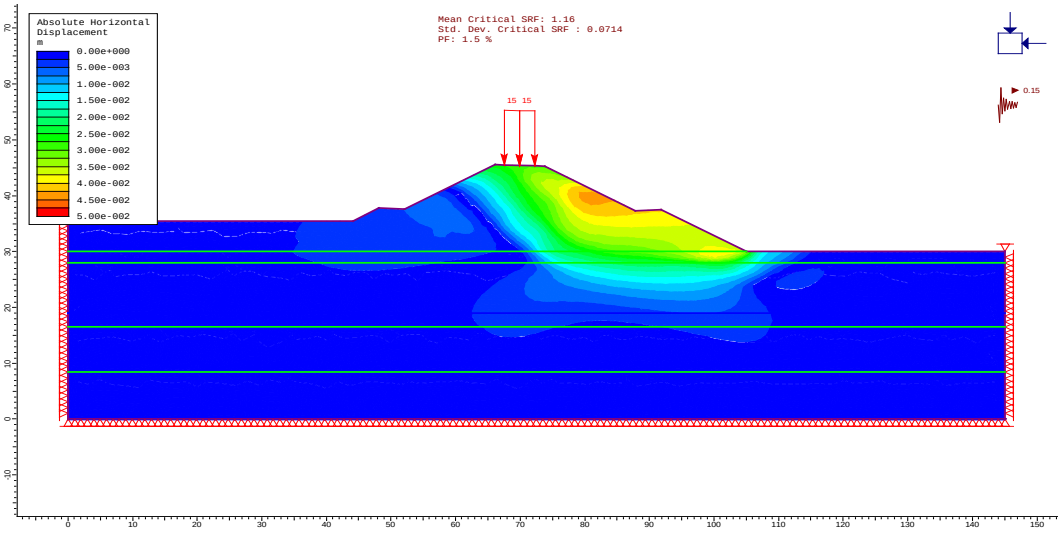

Figure 17: Absolute horizontal displacement using Phase^2 v8.0

Dynamic analysis using FLAC

Before evaluating the seismic response of the railway embankment, a factor-of-safety calculation was done as a check on the stability condition at this state (Figure 18). This is considered to be the state of the railway embankment at the time of the earthquake event (F=2.01).

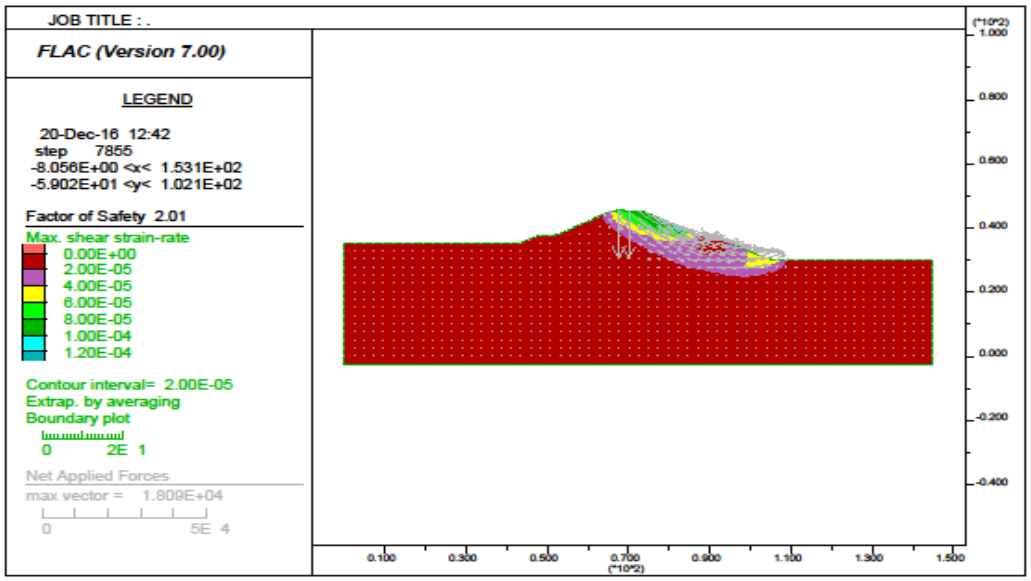

Figure 18: Factor-of-safety plot for railway embankment before earthquake occurred

The maximum shear strain contours throughout the model are plotted for Mohr-Coulomb material and Rayleigh damping and Byrne material and Rayleigh damping in Figure 19 and Figure 20 respectively. Movement of the railway embankment after 50 seconds is primarily concentrated along the left and right side of the slope face. This is clearly shown in the shear-strain increment contour plot.

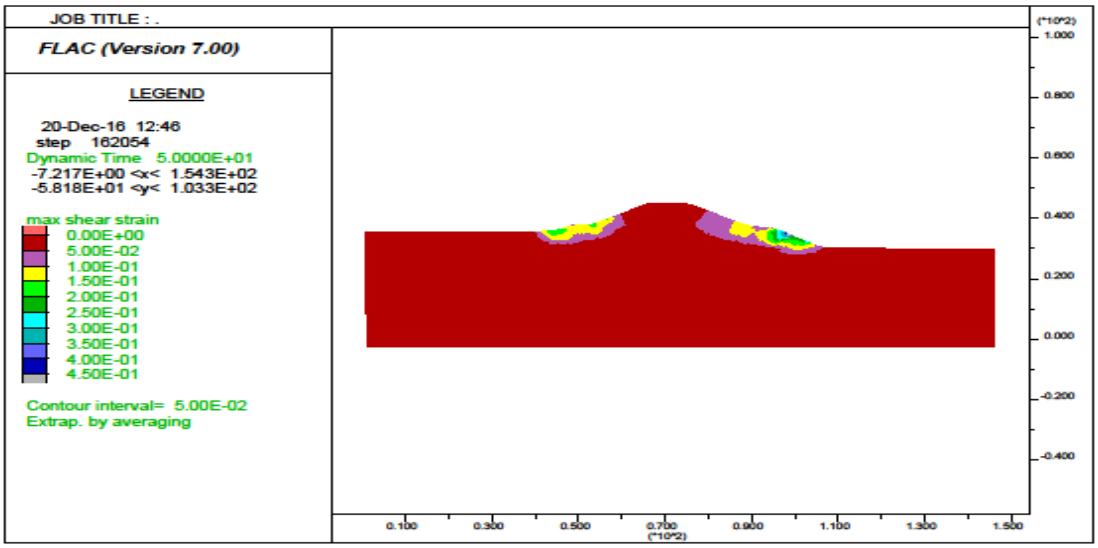

Figure 19: Shear-strain increment contours at 50 seconds– Mohr-Coulomb material and Rayleigh damping

As it can be seen from Figure 20, the Finn-Byrne model produced noticeable deformations along the lateral (free-field) boundaries of the model. Actually in Dynamic Analysis, the free field boundary performs a small-strain calculation even though the main grid is executing in large strain mode. In order to reduce the mismatch between large-strain and small-strain calculations, the lateral boundaries could be moved farther out. However, this will increase the simulation time.

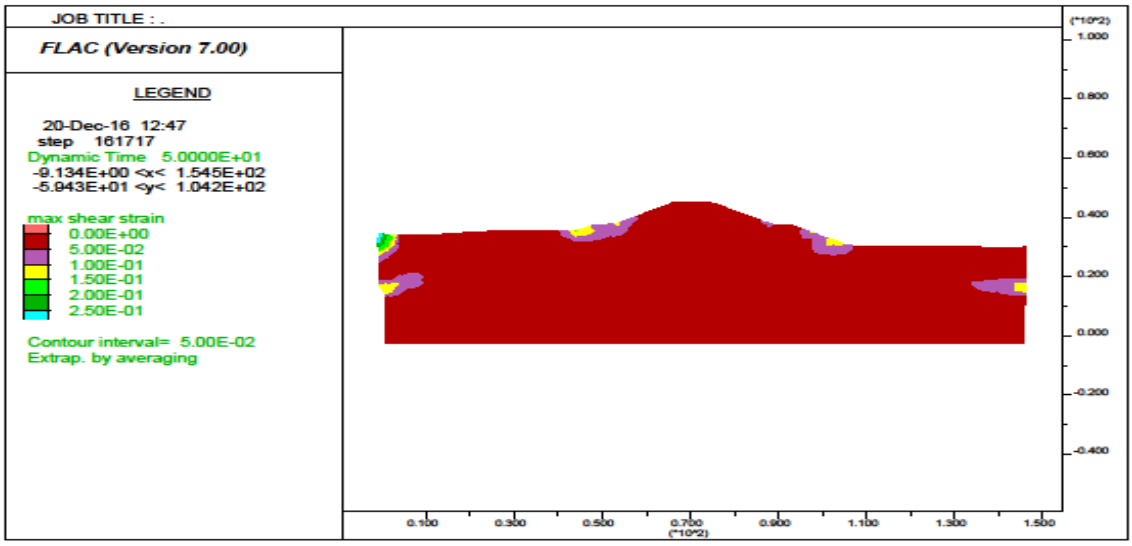

Figure 20: Shear-strain increment contours at 50 seconds – Byrne (liquefaction) material and Rayleigh damping Liquefaction

Figure 21 shows the pore pressure/effective stress measurement at grid point (23, 9), which is nearly at the middle of layer II. Increase in pore pressure (and decrease in effective stress) was observed at this point.

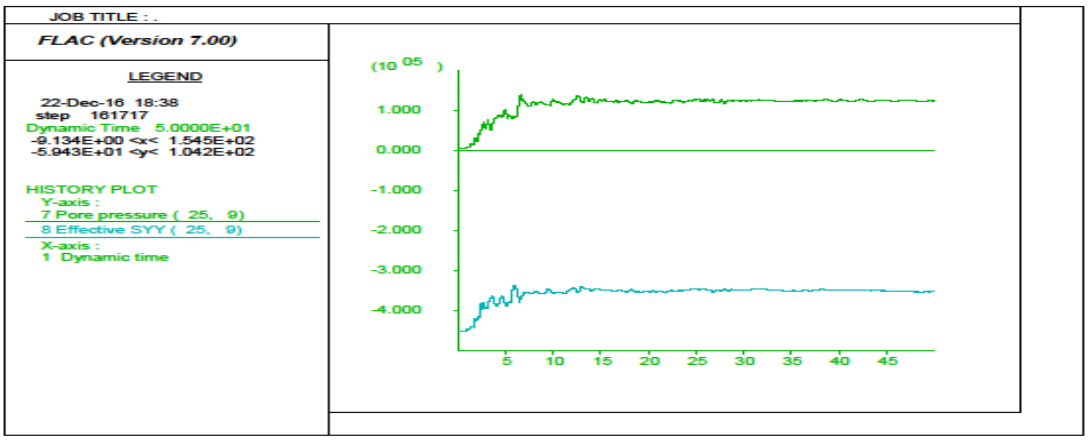

Figure 21: Pore-pressure and effective vertical stress near the middle of layer II – Byrne (liquefaction) material and Rayleigh damping

The normalized excess pore-pressure ratio (or cyclic pore-pressure ratio), u_e/σ_c, can be used to identify the region of liquefaction in the model, where u_e is the excess pore pressure and σ_c is the initial effective confining stress. A liquefaction state is assumed to occur when $u_e/\sigma_c = 1$. The excess pore-pressure ratio was calculated in *FISH* function "GETEXCESSPP.FIS," and the maximum value was stored in *FISH* extra array ex 6. However, for this railway embankment there was no any indication for liquefaction (Figure 22). This is attributed to stiff clay foundation soils and deep ground water table. Liquefaction occurs only in saturated soils, so the depth to groundwater (either free or perched) influences liquefaction susceptibility. Liquefaction susceptibility decreases with the increasing ground water depth [14]. At sites where groundwater levels fluctuate significantly, liquefaction hazards may also fluctuates

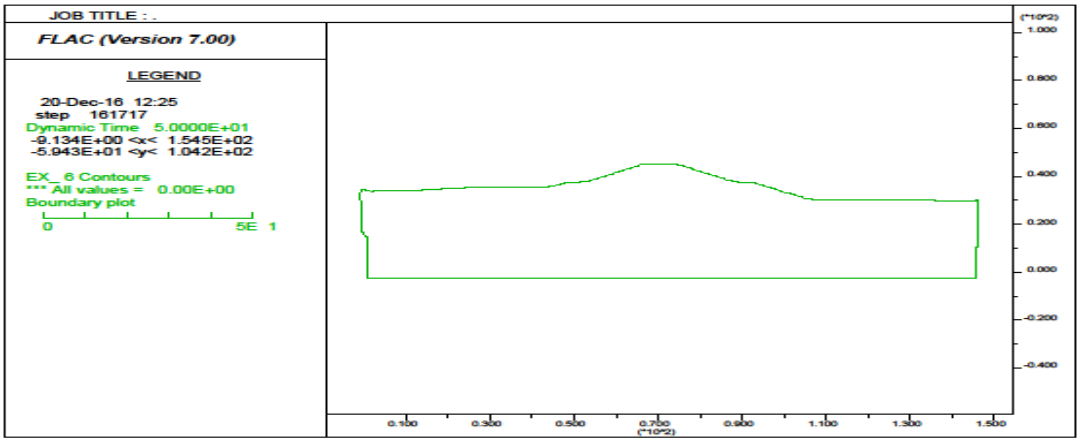

Figure 22: Excess pore-pressure ratio contours (values greater than 0.99) –Byrne (liquefaction) material and Rayleigh damping

CONCLUSIONS

In the preceding pages an attempt has been made to evaluate the slope stability of the new railway embankment found in Ethiopia; using three different stochastic approach together with commercially available finite element and finite difference programs. The main purpose of using reliability models

is its capability for becoming an effective mechanism in decision-making process. Probabilistic assessment is more efficient than deterministic methods which are solely relied on the safety factor. The first order reliability method (FORM), Monte Carlo Simulation (MCS) and Point-estimate method (PEM) gave 3.2%, 4.14% and 1.5% of probability of failure respectively. In the mean time, there was no any indication of liquefaction observed due to stiff foundation clay soils and deep groundwater table. For this railway embankment, *pseudo-static* analyses of the earthquake loading can be used, since there is no considerable strength loss by the cyclic loading. Knowing that, dynamic analyses are very complex, involve considerable uncertainties.

ACKNOWLEDGMENT

This research was supported by the National Natural Science Foundation of China (Grant Nos 51309141 and 51479102) and Public welfare Industry Special Fund of Ministry of Water Resources for Scientific Research Projects of China (Grant No. 201401029). The authors would like to acknowledge Engineer Abdulkerim Mohammed, Abdullah Kılıc, Bahadır Sonmez, Dr. Kıvanc Oklap and Suha Abik for their indispensable cooperation.

REFERENCES

1. J. Michael Duncan and Stephen G. Wright (2005). “Soil Strength and Slope Stability”. John Wiley & Sons Inc, pp. 293.
2. Abramson, L.W., Lee, T.S., Sharma, S., and Boyce, G.M. (2002). “Slope Stability and Stabilization Methods”. John Wiley & Sons Inc, pp.712.
3. Eleyas Assefa, Dr. Li Jian Lin, Dr. Costas I. Sachpazis, Dr. Deng Hua Feng, Dr. Sun Xu Shu, and Dr. Anthimos Anastasiadis (2016). “Discussion on the Analysis, Prevention and Mitigation Measures of Slope Instability Problems: A case of Ethiopian Railways”. Electronic Journal of Geotechnical Engineering, vol. 21.12, pp 4101-4119.
4. Phoon, K. K. and F. H. Kulhawy (1999). “Characterization of Geotechnical Variability”. Canadian Geotechnical Journal 36: 612-624.
5. Babu, G. L. S., A. Srivastava, et al. (2007). “Analysis of Stability of Earthen Dams in Kachchh Region, Gujarat, India”. Engineering Geology 94: 123-136.
6. Gregory B. Baecher and John T. Christian (2003). “Reliability and Statistics in Geotechnical Engineering”. John Wiley & Sons Inc, pp. 569.
7. Elkateb, T., R. Chalatumyk, et al. (2003). “An Overview of Soil Heterogeneity: Quantification and Implications on Geotechnical Field Problems.” Canadian Geotechnical Journal 40: 1-15.
8. Nemčok, A., Pašek, J. and Rybář, J. (1972). “Classification of landslides and other mass movements” Rock Mechanics, 4: 71-78.
9. Varnes, D. J. (1978). “Slope movements: types and processes. In: Schuster, R.L. and Krizek, R.J. (eds.) Landslide analysis and control”. National Academy of Sciences, Transportation Research Board Special Report 176, Washington, 11-33.
10. Hutchinson, J. N. (1988). “General report: Morphological and geotechnical parameters of landslides in relation to geology and hydrology”. In: Proc. 5th International Symposium on Landslides, Lausanne, 1: 3-35.
11. Cruden, D. M. and Varnes, D. J. (1996). “Landslide types and processes. In: Turner, A.K. and Schuster, R.L. (eds.) Landslides, Investigation and Mitigation”. Transportation Research Board Special Report 247, Washington D.C., 36-75.

12. Eleyas Assefa, Dr. Li Jian Lin, Dr. Costas I. Sachpazis, Dr. Deng Hua Feng, Dr. Sun Xu Shu, and Dr. Anthimos S. Anastasiadis (2016). "Probabilistic Slope Stability Evaluation for the New Railway Embankment in Ethiopia". Electronic Journal of Geotechnical Engineering, vol. 21.11, pp 4247-4272.
13. FLAC and ICG Inc. (2011). "FLAC: Fast Lagrangian Analysis of Continua User's Guide". Itasca Consulting Group Inc., Minneapolis.
14. Kramer, S.L. (1996). "Geotechnical Earthquake Engineering". Prentice Hall, pp. 437.
15. Robert W. Day (2002). "Geotechnical Earthquake Engineering Handbook". McGraw-HILL, pp. 572.
16. Seed H.B., Tokimatsu, K., L.F., and Chung, R. (1985). "Influence of SPT Procedures in Soil Liquefaction Resistance Evaluations". J. Geotechnical Eng'g, ASCE, 111(12), 861- 878.
17. Zhu, S.G. (1981). "Influence of Fines on Evaluating Liquefaction of Sand by CPT". Proc. Int. Conf. on Recent Advances in Geotechnical Eng'g, St. Louis, Missouri, 1: 167-172.
18. Zhou, S.G. (1987). "Soil Liquefaction during Recent Major Earthquakes in China and Seismic Design Method Related to Soil Liquefaction". Proc. 8th Asian Regional Conference on SM&FE, Vol. II, pp. 249-250.
19. Ishihara, K. (1993). "Liquefaction of natural deposits during earthquakes". Proc. 11th ICSMFE, SanFrancisco, 1, 321-376 Vol. 2, pp. 683-692.
20. Seed, R.B., Cetin, K.O., Moss, R.E.S., Kammerer, A. M., Wu, J., Pestana, J.M. and Riemer M.F. (2001). "Recent Advances in Soil Liquefaction Engineering and Seismic Site Response Evaluation", Proc. 4th Int. Conf. on Recent Adv. in Geotech. Earth. Eng'g and Soil Dynamics, San Diego.
21. Finn, W. D.L., Ledbetter, R. H., R.L. Fleming, R.L., Jr., Templeton, A.E., Forrest, T.W., and Stacy, S.T. (1994). "Dam on Liquefiable Foundation: Safety Assessment and Remediation" Proc. 17th International Congress on Large Dams, Vienna, pp. 531-553.
22. Bray, Jonathan D., Sancio, R.B., Reimer, M.F. and Durgunoglu, T. (2004). "Liquefaction Susceptibility of Fine grained Soils". Proc. 11th Int. Conf. On Soil Dynamics and earthquake Engineering and 3rd Inter. Conf. on Earthquake Geotech. Eng'g, Berkeley, CA, Jan. 7-9, Vol. 1, pp. 655-662.
23. Boulanger, Ross W. and Idriss, I.M. (2005), "New Criteria for distinguishing Between Silts and Clays That Are Susceptible to Liquefaction versus Cyclic failure". 25th. Annual USSD Conference, Salt Lake City, Utah, June 6-10, pp 357-366.
24. Idriss, I.M. and Boulanger, R.W. (2008). "Soil Liquefaction during Earthquakes", EERI, MNO-12.
25. Towhata, I. (2008), "Geotechnical Earthquake Engineering". Springer Series in Geomehanics and Geoengineering.
26. Shamsher Prakash and Vijay K. Puri (2010). "Recent Advances in Liquefaction of Fine Grained Soils". Fifth International Conference on Recent Advances in Geotechnical Earthquake Engineering and Soil Dynamics, Paper No. 4.17a, pp. 6.
27. GEO-SLOPE International Ltd. (2008). "Stability Modeling with SLOPE/W 2007 Version an Engineering Methodology". GEO-SLOPE International Ltd, Fourth Edition, pp. 347.

28. D.G. Fredulund and H. Rahardjo (1993). “Soil Mechanics for Unsaturated Soils”. John Wiley & Sons Inc, pp. 490.

29. Matsui, T., San, K. C. (1992). “Finite element slope stability analysis by shear strength reduction technique”. Journal of Soils and Foundation, 32: 59-70.

30. Griffiths, D. V., and Lane, P. A. (1999). “Slope stability analysis by finite elements”. Geotechnique 49(3), 387–403.

31. Zienkiewicz, O. C., C. Humpheson, et al. (1975). “Associated and non-associated Viscoplasticity and plasticity in soil mechanics.” Geotechnique 25: 671-689.

32. Naylor, D. J. (1981). “Finite elements and slope stability. Numerical methods in Geomechanics”. Proceedings of the NATO Advanced Study Institute, Lisbon, Portugal

33. Donald, I. B. and S. K. Giam (1988). “Application of the nodal displacement method to slope stability analysis”. Proceedings of the 5th Australia-New Zealand Conference on Geomechanics, Sydney, Australia

34. Dawson, E. M., Roth, W. H., Drescher, A. (1999). “Slope stability analysis by strength reduction”. Geotechnique, 49(6): 835-840.

35. Dawson, E. M. and W. H. Roth (1999). “Slope stability analysis with FLAC.” Flac and Numerical Modeling in Geomechanics: 3-9.

36. Hynes-Griffin, M. E., and Franklin, A. G. (1984). “Rationalizing the seismic coefficient method”. Final Report, Miscellaneous Paper GL-84-13, Department of the Army, U.S. Army Corps of Engineers, Waterways Experiment Station, Vicksburg, MS.

37. Marcuson, W. F., Hynes, M. E., and Franklin, A. G. (1990). “Evaluation and use of residual strength in seismic safety analysis of embankments”. Earthquake Spectra, Earthquake Engineering Research Institute, 6(3), 529–572.

38. Matsuo, M., Kuroda, K. (1974). “Probabilistic approach to design of embankments”. Soils and Foundations, 14(2): 1-17.

39. Alonso, E. E. (1976). “Risk analysis of slopes and its application to slopes in Canadian sensitive clays”. Geotechnique, 26(3): 453-472.

40. Chowdhury, R. N. (1984). “Recent developments in landslide studies: probabilistic methods [A]”. In proceedings of the 4th International Symposium on Landslides [C], Toronto, Ont., September 16-21. Canadian Geotechnical Society, 1: 209-228.

41. Wolff, T. F. (1985). “Analysis and design of embankment dam slopes: a probabilistic approach”. Ph.D. thesis, Purdue University.

42. Christian, J. T., Ladd, C. C., Baecher, G. B. (1994). “Reliability and probability in stability analysis”. Journal of Geotechnical Engineering, ASCE, 120(12): 1071-1111.

43. Malkawi, A. I. H., Hassan, W. F., Abdulla, F. A. (2000). “Uncertainty and reliability analysis applied to slope stability”. Journal of Structural Safety, 22(2): 161-187.

44. Low, B. K., Gilbert, R. B., Wright, S. G. (1998). “Slope reliability analysis using generalized method of slices”. Journal of Geotechnical and Geoenvironmental Engineering, 124(4): 350-362.

45. John T. Christian (2004). “Geotechnical Engineering Reliability: How Well Do We Know What We Are Doing?” Journal of Geotechnical and Geo-environmental Engineering, 130(10), 985-1003.

46. Moore, R. E. (1996). “Interval analysis”. Prentice-Hall, Englewood Cliffs, NJ.

47. Goodman, I. R., Nguyen, H. T. (1985). “Uncertainty models for Knowledge-based Systems; A Unified Approach to the Measurement of Uncertainty”. New York, Elsevier Science Inc.

48. Foye, K. C., Salgado, R., and Scott, B. (2006). “Assessment of variable uncertainties for reliability-based design of foundations”. Journal of Geotechnical and Geoenvironmental Engineering, 132(9).

49. Christian, J. T., and Baecher, G. B. (2001). Discussion on “Factors of safety and reliability in geotechnical engineering by J. M. Duncan,” Journal of Geotechnical and Geoenvironmental Engineering, 127(8), 700–702.

50. Harr, M. E. (1987). “Reliability-Based Design in Civil Engineering”. McGraw-Hill, New York.

51. Achintya Haldar and Sankaran Mahadevan, 2000. Probability, Reliability, and Statistical Methods in Engineering Design. John Wiley & Sons, Inc, pp.296.

52. Fishman, G. S. (1995). “Monte Carlo: Concepts, Algorithms, and Applications”. Springer, New York.

53. Gordon A. Fenton and D.V. Griffiths (2008). “Risk assessment in Geotechnical Engineering”. John Wiley & Sons Inc, pp. 435.

54. Rashad. Elrawy A. (2015). “Practical Application of Stochastic Methods in Geotechnical Engineering”. Journal of Engineering Sciences, Assiut University Faculty of Engineering, Pp57-70.

55. Box, G.E.P. and Muller, M.E. (1958). A note on “the generation of random normal deviates”. Annals of Mathematical Statistics, 29(2): 610-611.

56. Rocscience Inc. (2016). “Probabilistic analyses in Phase 2 8.0”. Accessed on 09/15/2016, https://www.rocscience.com/help/phase2/webhelp/phase2.htm.

57. Gustavo A. Ordonez (2011). “SHAKE2000 a Computer Program for the 1D-Analysis of Geotechnical Earthquake Engineering Problems User’s Manual”. pp. 231.

58. L.H. Mejia and E.M. Dawson, 2006. Earthquake deconvolution for FLAC. 4th International FLAC Symposium on Numerical Modeling in Geomechanics, Paper: 04-10, pp. 9.

Editor’s note.
This paper may be referred to, in other articles, as:

Eleyas Assefa, Dr. Li Jian Lin, Dr. Costas I. Sachpazis, Dr. Deng Hua Feng, Dr. Sun Xu Shu, and Xiaoliang Xu: “Slope Stability Evaluation for the New Railway Embankment using Stochastic Finite Element and Finite difference Methods” *Electronic Journal of Geotechnical Engineering*, 2017 (22.01), pp 51-79. Available at ejge.com